may have decreased in Japan throughout the period surveyed in this study[16]. Improvements in blood pressure control during this period are a possible reason for this reduction[16]; however, the increase in HDL demonstrated in this study may be an additional factor causing this change. If there is a prolonged effect of HDL elevation in reducing CHD, further effects of this trend may become apparent in the near future. It is important to confirm whether this increasing tread is a reality in Japan, determine what caused this large change and identify the possible consequences for Japanese public health.

Acknowledgment

The authors are grateful to Dr. Kazumasa Yamagishi at the University of Tsukuba and Dr. Hiroyasu Iso at Osaka University for their helpful discussion. They also thank Dr. Kunihiro Nishimura at NCVC and Dr. Hidenori Arai at Kyoto University for kindly providing background information for the data analysis.

Funding Sources

MEXT-Supported Program for the Strategic Research Foundation at Private Universities (Japan), Grant-in-aid from MEXT Japan.

Conflict of Interest Disclosure

None.

References

1) Huxley RR, Barzi F, Lam TH, Czernichow S, Fang X, Welborn T, Shaw J, Ueshima H, Zimmet P, Jee SH, Patel JV, Caterson I, Perkovic V, Woodward M: Isolated low levels of high-density lipoprotein cholesterol are associated with an increased risk of coronary heart disease: an individual participant data meta-analysis of 23 studies in the Asia-Pacific region. Circulation, 2011; 124: 2056-2064
2) Katanoda K, Matsumura Y: National Nutrition Survey in Japan--its methodological transition and current findings. J Nutr Sci Vitaminol (Tokyo), 2002; 48: 423-432
3) Katanoda K, Nitta H, Hayashi K, Matsumura Y: Is the national nutrition survey in Japan representative of the entire Japanese population? Nutrition, 2005; 21: 964-966
4) Yamamoto A, Nakamura H, Yasugi T, Mabuchi H, Kita T, Matsuzawa Y, Nakaya N, Saito S, Horibe H: Current state of and recent trends in serum lipid levels in the general Japanese population. Research Committee on Serum Lipid Level Survey 1990 in Japan. J Atheroscler Thromb, 1996; 2: 122-132
5) Arai H, Yamamoto A, Matsuzawa Y, Saito Y, Yamada N, Oikawa S, Mabuchi H, Teramoto T, Sasaki J, Nakaya N, Itakura H, Ishikawa Y, Ouchi Y, Horibe H, Kita T: Serum lipid survey and its recent trend in the general Japanese population in 2000. J Atheroscler Thromb, 2005; 12: 98-106
6) Kadono A, Yamagishi K, Sankai T, Umesawa M, Cui R, Imano H, Ohira T, Kiyama M, Kitamura A, Wakabayashi Y, Nakamura M, Iso H: A 20-year trends in serum HDL-cholesterol in a community: The CIRCS Kyowa Study (abstract) [in Japanese] J Epidemiol 2013; 23 (suppl 1): 96
7) Miida T, Nishimura K, Okamura T, Hirayama S, Ohmura H, Yoshida H, Miyashita Y, Ai M, Tanaka A, Sumino H, Murakami M, Inoue I, Kayamori Y, Nakamura M, Nobori T, Miyazawa Y, Teramoto T, Yokoyama S: A multicenter study on the precision and accuracy of homogeneous assays for LDL-cholesterol: Comparison with a beta-quantification method using fresh serum obtained from non-diseased and diseased subjects. Atherosclerosis, 2012; 225: 208-215
8) Dati F, Tate J: Reference Materials for the Standardization of the Apolipoproteins A-I and B, and Lipoprotein(a). eJ Int Fed Clin Chem, 2002; 13: http://www.ifcc.org/ifcc-files/docs/1303200103.pdf
9) Sugiuchi H, Uji Y, Okabe H, Irie T, Uekama K, Kayahara N, Miyauchi K: Direct measurement of high-density lipoprotein cholesterol in serum with polyethylene glycol-modified enzymes and sulfated alpha-cyclodextrin. Clin Chem, 1995; 41: 717-723
10) Huang YC, Kao JT, Tsai KS: Evaluation of two homogeneous methods for measuring high-density lipoprotein cholesterol. Clin Chem, 1997; 43: 1048-1055
11) Sakai Y, Itakura K, Kanada T, Ebata N, Suga K, Aikawa H, Nakamura K, Sata T: Quantitation of apolipoprotein A-I in pooled human serum by single radial immunodiffusion and sodium dodecyl sulfate-polyacrylamide gel electrophoresis. Anal Biochem, 1984; 137: 1-7
12) Carroll MD, Kit BK, Lacher DA, Shero ST, Mussolino ME: Trends in lipids and lipoproteins in US adults, 1988-2010. JAMA, 2012; 308: 1545-1554
13) Carroll MD, Lacher DA, Sorlie PD, Cleeman JI, Gordon DJ, Wolz M, Grundy SM, Johnson CL: Trends in serum lipids and lipoproteins of adults, 1960-2002. JAMA, 2005; 294: 1773-1781
14) Schaefer EJ: Lipoproteins, nutrition, and heart disease. Am J Clin Nutr, 2002; 75: 191-212
15) Matsumura Y: Nutrition trends in Japan. Asia Pac J Clin Nutr, 2001; 10 Suppl: S40-47
16) Ueshima H: Explanation for the Japanese paradox: prevention of increase in coronary heart disease and reduction in stroke. J Atheroscler Thromb, 2007; 14: 278-286

Supplementary Table 1. Number of case samples (n) for HDL-C in each study

	NHNS		SRL		Hiroshima		Niigata		BQ		NCUH		NCVCH		CIRCS	MHLWJ
Year	Male	Female	Male	Female	Male	Female	Male	Female	Male	Female	Male	Female	Male	Female	Ref. 6	Ref. 4 and 5
1984			983	983												
1985			1205	1071												
1986			1168	935												
1987			1242	980												
1988			848	882												
1989	2750	4167	4056	5393												
1990	3371	4745	6352	7215												
1991	3521	5033	8062	8512												
1992	2940	4303	10960	11274												
1993	2618	3917	10321	10632							23492	27772				
1994	2083	3279	11597	11180			181782	86779			24007	27857				
1995	1823	2975	7080	7980			178522	85308			22372	26210				
1996	2209	3431	5461	6006			181103	88378			9194	9169				
1997	2503	3797	5444	6999	1337	660	185679	88719			9142	7827				
1998	2691	4029	6401	9142	1360	598	176125	86221			7845	7446				
1999	2293	3591	7767	9449	1525	749	170871	82774			7813	7483				
2000	2316	3326	3584	3199	1444	653	168874	83892			7820	7671				
2001	2126	3357	2324	1802	1490	703	169774	82827			8514	8647				
2002	2124	3183	2708	2640	1473	681	162309	78926			8967	9153				
2003	2078	3151	2041	2375	1505	704	146517	72089			11874	13171				
2004	1220	1912	1629	1384	1577	751	145241	71123			9396	10154				
2005	1521	2273	1447	1280	1523	711	146498	69303			9952	10199	20833	13451		
2006	1703	2504	1184	941	1687	714	143343	69010			14187	14575	21264	14629		
2007	1602	2368	918	952	1560	777	144260	71409			17417	18000	13934	10447		
2008	1817	2630	1192	952	1368	547	150931	79452			19652	19806	32969	20856		
2009	1738	2558	905	727	1130	415	145893	79337			23289	23033	35307	20378		
2010			1097	824	1102	411	142370	78465	36	26	26149	26095	37175	20724		
2011			869	614			141558	79224			26749	26369	39423	22589		
2012											28980	27858	27696	16261		

Supplementary Table 2. Number of case samples (n) in the apoA-I study

Year	SRL apoA-I	
	Male	Female
1984	286	227
1985	512	525
1986	650	723
1987	983	1185
1988	1203	1339
1989	1568	1881
1990	2363	2890
1991	3226	3472
1992	3458	4005
1993	3130	3439
1994	3152	3519
1995	3563	3500
1996	3355	3402
1997	2562	2376
1998	2902	2904
1999	2625	2615
2000	2748	2618
2001	1994	2114
2002	2008	2021
2003	1554	1541
2004	1727	1589
2005	1932	1595
2006	1699	1514
2007	2103	1888
2008	2078	1681
2009	2411	1931
2010	2619	1870
2011	2772	1866

Supplementary Table 3. Assay systems, Reagents and CDC or other Standardization

Year	SRL							Niigata	NCUH
	HDL-C (CDC)				ApoA-I (International Standardization)			HDL-C (CDC)	HDL-C (CDC)
	Reagent	System	Standard	Correlation*	Reagent	System	Correlation	Reagent	Reagent
1984	W-MnCL	Technicon AA			SRID				
1985					ApoA-I Auto Daiichi	Cobas	y=0.96x+1.13, r=0.974		
1986	Heparin-Ca		Preiset Cholestrin	y=0.96x+1.02, r=0.992					
1987		H705		y=1.04x−1.37, r=0.995					
1988						H7150	y=0.98x+1.0, r=0.974		
1989									
1990									
1991		H7150		y=0.97x+2.06, r=0.998					
1992									
1993									
1994									
1995						H7170	y=0.99x+2.5, r=0.988		
1996	HDL-C Auto Daiichi	H7170	HDL-C Auto CAL	y=0.95x+4.9, r=0.994					
1997	Choles Test HDL		Choles Test HDL CAL	y=0.99x−0.1, r=0.992	ApoA-I AutoN Daiichi		y=0.82x−0.55, r=0.998	Choles Test HDL	
1998						BM12	y=1.01x−0.554, r=0.998		
1999									
2000			ColesTest Calibrater	y=1.01x−0.0, r=0.992					Choles Test N HDL
2001	Choles Test N HDL			y=0.98x+1.18, r=0.997				Choles-Test N HDL	
2002									Determi-ner LHDL
2003									
2004									Denka EX-N
2005									
2006									
2007		BM8060		y=1.003x+1.18, r=0.998					
2008						BM8040	y=1.03x−3.87, r=0.999		
2009									
2010									
2011									
2012									

The NCVCH and CIRCS data are qualified by CDC standardization.
*Validation for changing assay systems/reagents.

ANTICANCER RESEARCH *33*: 4237-4248 (2013)

Therapy with siRNA for *Vegf-c* but Not for *Vegf-d* Suppresses Wide-spectrum Organ Metastasis in an Immunocompetent Xenograft Model of Metastatic Mammary Cancer

MASA-AKI SHIBATA[1], EIKO SHIBATA[2], JUNJI MORIMOTO[3] and MARIKO HARADA-SHIBA[2]

[1]*Laboratory of Anatomy and Histopathology, Graduate School of Health Sciences, Osaka Health Science University, Kita-ku, Osaka, Japan;*
[2]*Department of Molecular Innovation in Lipidology, National Cerebral and Cardiovascular Center Research Institute, Suita, Osaka, Japan;*
[3]*Laboratory Animal Center, Osaka Medical College, Takatsuki, Osaka, Japan*

Abstract. *Cancer metastasis contributes significantly to cancer mortality and is facilitated by lymphangiogenesis and angiogenesis. Vascular endothelial growth factors-C and D (VEGF-C and VEGF-D) are heavily involved in lymphangiogenesis. Using small interfering RNA (siRNA) against mouse Vegf-c, and Vegf-d, we sought to inhibit metastasis in a model of metastatic murine mammary cancer. BJMC3879Luc2 cell-induced mammary carcinomas received direct intratumoral injections in vivo of either plasmid VEGF-C/D siRNA (psiVEGF-C, psiVEGF-D) or a vector control followed by in vivo gene electrotransfer weekly for seven weeks. Treatment with psiVEGF-C and with psiVEGF-D resulted in lower tumor volumes as compared to the controls. Treatment with psiVEGF-C suppressed wide-spectrum organ metastasis involving lung and lymph nodes. Treatment with psiVEGF-C further reduced the number of dilated lymphatic vessels with invading cancer cells and inhibited tumor blood microvessel density. In contrast, although treatment with psiVEGF-D was not effective and gave equivocal results, it did induce some insignificant reduction in tumor volume increment, average numbers of lymph node metastases and average number of intratumoral dilated lymphatic vessels. In conclusion, specific silencing of the Vegf-c gene suppresses wide-spectrum organ metastasis, including the lung and lymph nodes. However, therapy with siRNA for Vegf-d was not adequately effective in this murine system.*

Correspondence to: Professor M.A. Shibata, Laboratory of Anatomy and Histopathology, Graduate School of Health Sciences, Osaka Health Science University, 1-9-27 Temma, Kita-ku, Osaka 530-0043, Japan. Tel: +81 675069046, Fax: +81 663525995, e-mail: masaaki.shibata@ohsu.ac.jp

Key Words: siRNA, VEGF-C, VEGF-D, metastasis, mammary cancer.

Breast cancer is the most common malignant disease in women worldwide. According to the International Agency for Research on Cancer, an estimated 1,384,000 patients were diagnosed with breast cancer in 2008. In 2008, 458,000 women died of breast cancer worldwide (1). Perhaps more worrisome is the increasing incidence among younger women under 40 years of age (2-4). Breast cancer lethality is largely due to metastasis, preferentially to lymph nodes, lung and bone (5). In order to reduce both morbidity and mortality, less toxic, more effective chemopreventive and anti-metastatic treatments are desperately required.

Lymph node metastasis is one of the most important adverse prognostic factors for breast carcinoma (6). Members of the vascular endothelial growth factor (VEGF) family promote the formation of new blood and lymphatic vessels in tumor tissues, enabling the spread of tumor cells (7). Within the VEGF family, both VEGF-C and VEGF-D have been reported to induce lymphangiogenesis *via* activation of VEGF receptor-3 (VEGFR-3) expressed on lymphatic endothelial cells (8, 9). In animal models, VEGF-C and VEGF-D have also been shown to enhance lymphangiogenesis and associated lymphatic metastasis (10-16), while clinical studies showed an association of overexpression of either VEGF-C or VEGF-D with lymph node metastasis and poor prognosis in patients with breast cancer (17-20).

Using an immunocompetent mouse mammary cancer model, we previously demonstrated inhibition of Vegf-c and Vegf-a by gene silencing using vectors expressing short interfering RNA (siRNA) which led to suppression of lymphatic and/or hematogenous metastasis (21). Here we confirmed the anti-metastatic action of *Vegf-c* siRNA using a different siRNA sequence reported previously (21), and examined the effectiveness of silencing related *Vegf-d* by the same method.

0250-7005/2013 $2.00+.40

Materials and Methods

Cell line. The BJMC3879 mammary adenocarcinoma cell line was derived from a metastatic focus within a lymph node of an inoculated BALB/c mouse in an earlier study. When inoculated into BALB/c mice, the line continues to retain a high metastatic propensity, especially to lymph nodes and lungs (21-23). In addition, BJMC3879 cells have been reported to carry the *p53* mutation, as inferred by immunohistochemistry (24). The BJMC3879Luc2 mammary carcinoma cell line used in our investigations was generated by stable transfection of the *luc2* gene (an improved firefly luciferase gene) into the parent BJMC3879 cell line (25). BJMC3879Luc2 cells were maintained in RPMI-1640 medium containing 10% fetal bovine serum with streptomycin/penicillin at 37°C under 5% CO_2.

Animals. Thirty six-week-old female BALB/c mice (Japan SLC, Hamamatsu, Japan) were housed five per plastic cage on wood chip bedding with free access to water and food under controlled temperature (21±2°C), humidity (50±10%), and lighting (12-12 h light-dark cycle) conditions. All animals were held for a one-week acclimatization period before study commencement. This animal experiment was approved by the Animal Experiment Committee of Osaka Medical College (approved no. 19017). Mice were treated in accordance with the procedures outlined in the Guide for the Care and Use of Laboratory Animals at Osaka Medical College, the Japanese Government Animal Protection and Management Law (No.105) and the Japanese Government Notification on Feeding and Safekeeping of Animals (No.6).

siRNA sequences for silencing mouse Vegf-c or Vegf-d. Four different sequences each of siRNA oligonucleotides targeting *Vegf-c* and *Vegf-d*, were synthesized using the Qiagen kit and protocol (Qiagen, GmbH, Hilden, Germany). The four siRNA sequences for mouse *Vegf-c* were as follows: Vegf-C1, 5'-GAAUGACUAUAUAAUUUAUtt-3' and 5'-AUAAAUUAUAUAGUCAUUCtt-3'; Vegf-C2, 5'-CACAGAAGUGC UUCCUUAAtt-3' and 5'-UUAAGGAAGCACUUCUGUGtg; Vegf-C3, GACGUUGUUUGAAAUUACAtt-3' and 5'-UGUAA UUUC AAACAACGUCtt-3'; Vegf-C4, 5'-CAGGGAAUUUGAUG AGAA Utt-3' and 5'-AUUCUCAUCAAAUUCCCUGtt-3'. The four siRNA sequences for mouse *Vegf-d* were as follows: Vegf-D1, 5'-GGGCAAUGCUCAUGAGUUAtt-3' and 5'-UAACUCAUGAGC AUUGCCCtt-3'; Vegf-D2, 5'-CGCCAUCCUUACUCAAUUAtt-3' and 5'-ggCGGUAGGAAUGAGUUAAAU; Vegf-D3, 5'-CGAGUU AGUGCCUGUUAAAtt t-3' and 5'-UUUAACAGGCACU AACU CGgg-3'; Vegf-D4, 5'-GGAUAACACCAAAUGUAAAtt-3' and 5'-UUUACAUUUGGUGUUAUCCca-3'. The scrambled negative siRNA control was purchased from Qiagen.

Transfection of siRNAs into mammary cancer cells. BJMC3879Luc2 cells were plated in 24-well plates at 8×10^4 cells/well and transfected with 25 nM siRNA-Vegf-C1 to -C4, siRNA-Vegf-D1 to -D4 or 25 nM negative siRNA control using the Hyperfect transfection reagent (HyperFect; Qiagen). At 24 h post-transfection, cells were collected and total RNA extracted using an RNeasy Mini Kit (Qiagen). cDNAs were synthesized using a Transcriptor First Strand cDNA Synthesis Kit (Roche Diagnostics GmbH, Manheim, Germany). Real-time reverse transcription-PCR (RT-PCR) was performed using a LightCycler (Roche Diagnostics) as follows: an initial step at 95°C for 10 min, followed by 40 cycles of 10 s at 95°C, 10 s at 60°C, and 10 s at 72°C. The primer sequences for mouse *Vegf-c*, *Vegf-d* and *glyceraldehyde-3-phsophate dehydrogenase* (*Gapdh*) are shown in Table I. The relative mRNA levels of *Vegf-c* or *Vegf-d* were calculated using a $2^{-\Delta\Delta Ct}$ method (26) which is based on the fact that the difference in threshold cycles (ΔCt) between *Vegf-c* or *Vegf-d* and *Gapdh* internal control is proportional to the relative expression level of the gene of interest.

siRNA expression vectors. To construct short hairpin RNAs (shRNA) targeting mouse *Vegf-c* or *Vegf-d*, the following oligonucleotides were designed: Vegf-C1 siRNA, 5'-GATCCGAATGAC TATATAATTTATtagtgctcctggttgATAAATTATATAGTCATTCTTTT TTA-3'; and Vegf-D1 siRNA, 5'-GATCCGGGCAATGCTC ATGAGTTAtagtgctcctggttgTAACTCATGAGCATTGCCCTTTTTT A-3'. The lower case letters in each sequence above indicate the 15-nucleotide spacer separating the antisense segments. Each complementary oligonucleotide was annealed and ligated into a pBAsi-mU6PurDNAvector (Takara Bio, Inc., Otsu, Japan). This vector contains an RNA polymerase III promoter, the mouse U6 promoter, which can generate high amounts of shRNAs. A control siRNA vector was also purchased from Takara Bio, Inc. This control siRNA vector contains a scrambled sequence with no homology to any human or mouse mRNA. The control siRNA sequence was as follows: 5'-GATCCGTCTTAATCGCGTATAAGGCtagtgctcctggttgG CCTTATACGCGATTAAGACTTTTTTA-3'. For simplicity, in this article, the therapeutic vectors are referred to as psiVEGF-C, psiVEGF-D, and psiSCR (scrambled control).

In vivo siRNA Vegf-c or Vegf-d gene therapy. We inoculated BJMC3879Luc2 cells (5×10^6 cells/0.3 ml in PBS) subcutaneously into the right inguinal region of 30 female BALB/c mice. The animals were then randomly allocated into three groups of 10 mice each, as the psiVEGF-C, psiVEGF-D or psiSCR (control) groups. Two weeks post-inoculation, when the resulting tumors had reached 0.3-0.5 cm in diameter, we injected psiVEGF-C, psiVEGF-D or psiSCR (0.5 μg/μl saline) directly into the tumors using a 27-gauge needle while the animals were under isoflurane anesthesia. *In vivo* gene electrotransfer was performed immediately after by applying a conductive gel (Echo Jelly; Aloka Co., Ltd., Tokyo, Japan) topically to the unshaved skin over the tumor and to the surface of small platinum 'forceps' electrode plates. Electric pulses were then delivered directly into the tumor *via* these plate electrodes (CUY650-10; Nepa Gene Co., Ltd., Ichikawa, Japan) using a CUY21EDIT square-wave electropulser (Nepa Gene Co., Ltd.) generating 8 pulses with a pulse length of 20 milliseconds at 100 volts (22, 27-29). Vector injection and gene electrotransfer were performed once a week for seven weeks. As the tumors grew, a volume of ≤150 μl of vector solution was introduced into larger masses, while smaller tumors of 0.6-0.7 cm in diameter were infused until we detected leakage of the vector solution. We hoped to reliably administer of 50-75 μg plasmid/tumor, dependent on tumor size.

Using calipers, we measured the size of each treated mammary tumor weekly and calculated tumor volumes using the formula: maximum diameter × (minimum diameter)^2 ×0.4 (30). Individual body weights were also recorded at weekly intervals. After seven weeks of treatment, all mice were euthanized and the mammary tumors and certain lymph nodes (*i.e.* nodes from axillary and femoral regions, as well as any that appeared abnormal) were removed. We then immediately fixed a portion of each tissue sample in 10% phosphate-buffered formalin and processed through to paraffin embedding; an additional portion of each tumor was also

Table I. *Primer sequences for RT-PCR analysis.*

Genes	Primer sequences (5'-3')	PCR products (bp)
Vegf-c	F: AACGTGTCCAAGAAATCAG	157
	R: TGGATCACAATGCTTCAGT	
Vegf-d	F: ACTTGGTGCAGGGCTTCAGG	165
	R: CATCGCCACAGCTTCCAGTC	
Gapdh	F: TGGCCTTCCGTGTTCCTACC	135
	R: AGCCCAAGATGCCCTTCAGT	

F: Forward, R: reverse.

immediately frozen in liquid nitrogen for molecular analysis. Lungs were routinely inflated with the fixative, excised, and immersed in the fixative. We subsequently trimmed and examined all lobes for metastatic foci before processing for histology, where they were cut into 4-μm slices and stained with hematoxylin and eosin (H&E) for histopathological examination.

In vivo bioluminescent imaging. At experimental week 7, we anesthetized four or five mice from each group using isoflurane inhalation administered *via* the SBH Scientific anesthesia system (SBH Designs, Inc., Windsor, Ontario, Canada). Each anesthetized mouse received an intraperitoneal injection of 3 mg of D-luciferin potassium salts (Wako Pure Chemical Industries, Osaka, Japan) for bioluminescent screening with a Photon Imager (Biospace Lab, Paris, France). We quantified the bioluminescent signals received during the 6-min acquisition time with the Photovision software (Biospace Lab).

Histopathological analysis. All mice were euthanized and necropsied at week 7. Mammary tumors, lungs, lymph nodes, and abnormal organs/tissues were removed from each mouse, fixed in 10% phosphate buffered formaldehyde solution, paraffin- embedded and cut at 4 μm. Mounted tissue sections were stained with either H&E for histopathological examination or left unstained for immunohistochemical analysis. We routinely removed lymph nodes from the axillary and femoral regions, as well as any lymph nodes that appeared abnormal. Lungs were inflated with formaldehyde solution prior to excision and fixation and each lung lobe examined individually for metastatic foci prior to paraffin embedding.

Microvascular density in mammary tumors. We quantitatively assessed lymphatic and blood microvessel density in primary mammary carcinomas by immunohistochemistry (IHC) using the avidin-biotin complex (ABC) method (LSAB kit; Dako, Glostrup, Denmark) with hamster anti-podoplanin monoclonal antibody (AngioBio Co., Del Mar, CA, USA), a lymphatic endothelium marker, and rabbit anti-CD31 polyclonal antibody (Lab Vision Co., CA, USA), a specific marker for blood vessel endothelium. Since histological confirmation of lymphatic vessel invasion by tumor cells has prognostic value in various malignancies, we counted the number of podoplanin-positive lymphatic vessels containing intraluminal tumor cells and expressed them as the mean±SD. We additionally counted the number of CD31-positive blood microvessels by first scanning the slides at low magnification (×100) to locate areas of highest vessel density and then selecting five sites within those areas to count at higher magnification (×200-400). Values obtained were expressed as the mean±SD (31).

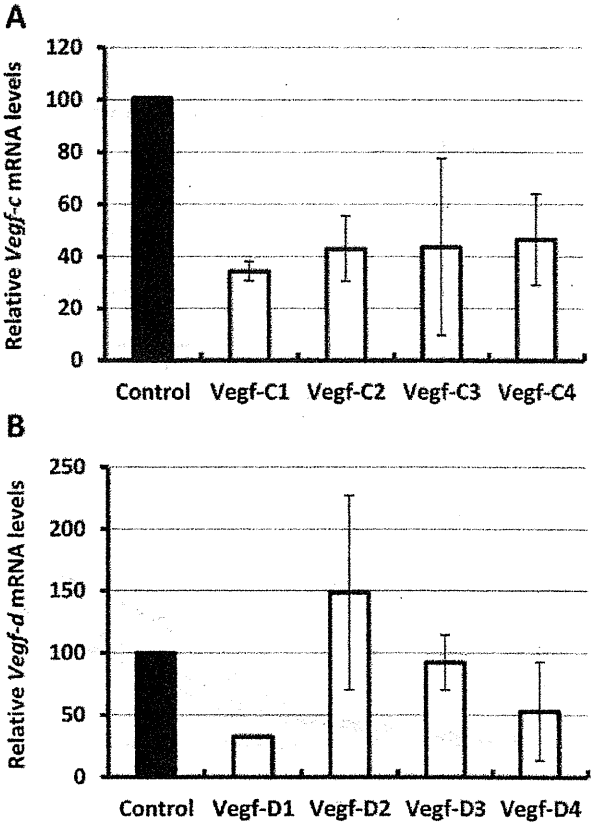

Figure 1. *Effectiveness of siRNA sequences targeted to vascular endothelial growth factor-C (Vegf-c) or Vegf-d. We transfected BJMC3879Luc2 mammary carcinoma cultures with four different sequences of siRNA oligonucleotides and measured the relative mRNA levels of Vegf-c (A) and Vegf-d (B) in mouse mammary carcinoma cells. As compared to the negative control siRNA, constructed from scrambled sequences, siRNA-Vegf-C1 reduced Vegf-c mRNA levels to 66% that of the control. The other siRNA constructs C2, C3, and C4 were less effective, lowering Vegf-c mRNA by 57%, 56%, and 53%, respectively siRNA-Vegf-d-D1 reduced Vegf-d mRNA levels to 67% to those of the control.*

Statistical analyses. Significant quantitative differences in intergroup data were analyzed using Welch's Student's *t*-test, which provides for insufficient homogeneity of variance. The variations in metastatic incidence were examined by Fisher's exact probability test, with $p<0.05$ or $p<0.01$ considered to represent a statistically significant difference.

Results

Selection of functional siRNA sequence for mouse Vegf-c or Vegf-d. Figures 1A and B illustrate the knockdown ratios of each *Vegf-c* and *Vegf-d* siRNA oligonucleotides tested in BJMC3879Luc2 cells. Out of the siRNAs targeted to these growth factors, the strongest silencing was achieved with oligonucleotides Vegf-C1 and Vegf-D1 (66% and 67% respectively).

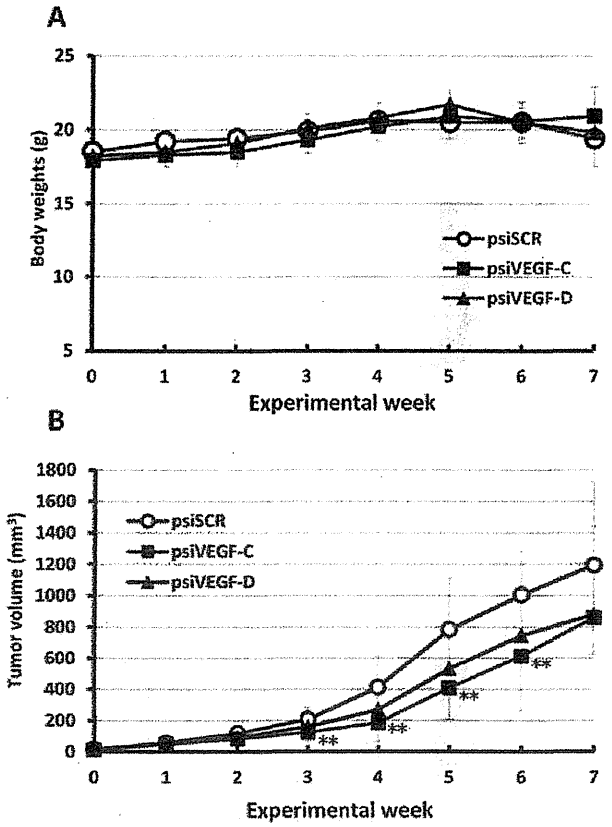

Figure 2. *Comparison of body weights and mammary tumor volumes in BALB/c female mice receiving intratumoral treatment with control psiSCR, psiVEGF-C or psiVEGF-D. A: Body weights were similar in all groups until the end of the study at seven weeks when mortality, which was greatest in psiSCR- and psiVEGF-D-treated mice, may have contributed to a slight decrease in those groups. B: From weeks 3-6, gains in tumor volumes were significantly suppressed in psiVEGF-C-transfected mice vs. psiSCR-treated controls. psiVEGF-D treatment tended to depress tumor volume increase throughout the study, but not to a statistically significant degree. Data represent the mean±SD. Although initial animal number was ten in each group, but survival number of animals at the end of the experiment was five in the psiSCR-treated group, nine in the psiVEGF-C-treated group and seven in the psiVEGF-D-treated group. All cause of death was due to cancer metastasis. *p<0.05; **p<0.01 compared to psiSCR-treated controls.*

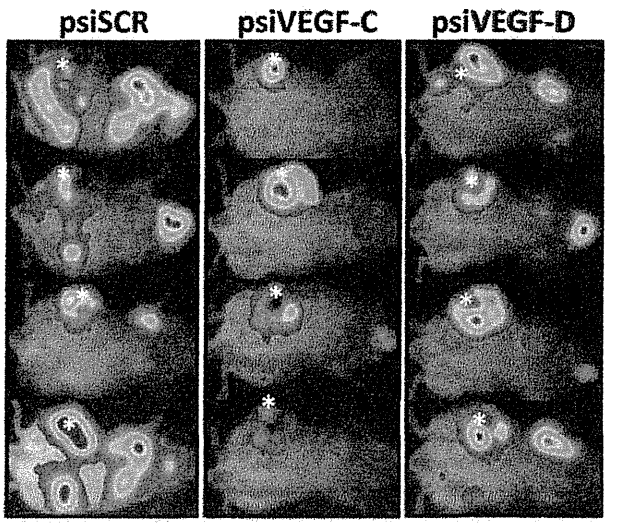

Figure 3. *Bioluminescent imaging at week 7 in four representative mice receiving control or targeted vascular endothelial growth factor-C (Vegf-c)/Vegf-d siRNA. Mammary tumors were generated by inoculating BMJC3879Luc2 cells, which were stably transfected with a luciferase gene, into the inguinal mammary pads. Bioluminescent signals were lowest in mice treated with psiVEGF-C, indicating markedly reduced metastasis, vs. mice receiving either control psiSCR or psiVEGF-D. However, there was also some signal reduction in the psiVEGF-D-treated mice compared to the controls.*

Body weights and tumor growth of animals under Vegf-c or Vegf-d siRNA treatment. At seven weeks, one animal from the psiVEGF-C group, and three animals from the psiVEGF-D group died due to metastasis *vs.* five animals in the control psiSCR group. As shown in Figure 2A, body weights did not differ statistically between all mice throughout the experiment until week 7, when there was a decrease in the weights of control and psiVEGF-D-treated animals (psiVEGF-C: 20.9±2.0 g; psiVEGF-D: 19.8±2.4 g; psiSCR: 19.4±1.9 g).

Tumor volumes are presented in Figure 2B. As compared to the psiSCR-treated mice, tumor volume increase in the psiVEGF-C-treated group significantly slowed from weeks 2 through 6. Increases in volumes of psiVEGF-D-treated tumors also tended to be lower in relation to controls, but the differences were not significant.

Bioluminescent imaging of transfected mice. Bioluminescent imaging revealed signals indicative of metastatic growth in mandibular, axillary, and inguinal lymphatic regions in all groups; however, less metastatic expansion occurred in mice from both the psiVEGF-C- and -D-treated groups as compared to control animals (Figure 3), with a more pronounced reduction in VEGF-C-treated mice.

Histopathological analysis of mammary tumors. Mammary tumors induced by BJMC3879Luc2 cell inoculations uniformly proved to be moderately-differentiated adenocarcinomas; we found no histopathological differences among groups. However, we did note treatment-induced variations in metastatic incidence and spread. Figure 4 summarizes the incidence and average number of metastatic lesions counted across multiple organs, and Figure 5 illustrates the histopathological presentation. Lymph node metastasis occurred in 100% of mice in the control psiSCR- and

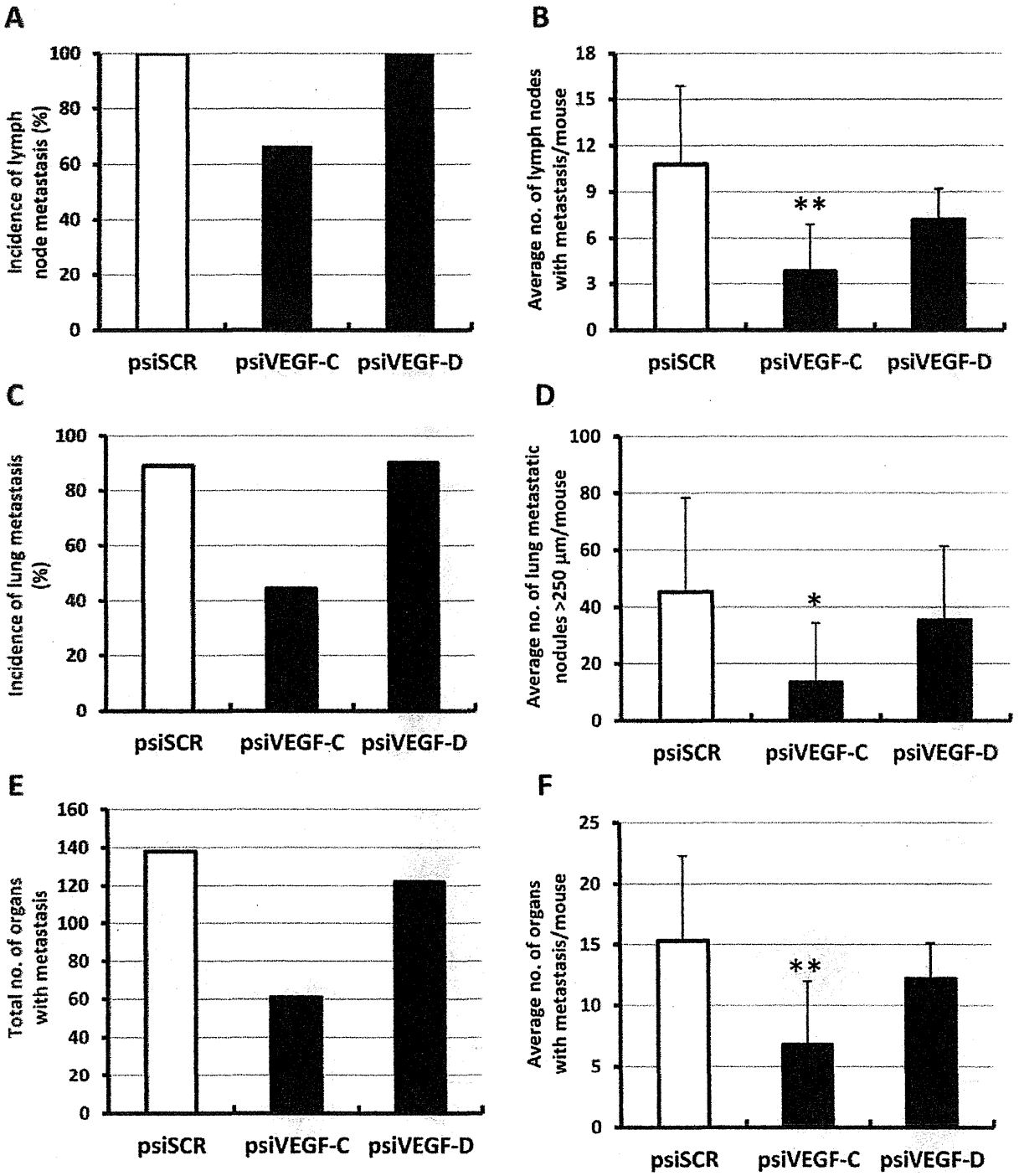

Figure 4. *Quantitative analysis of metastasis in lymph nodes, lung and other organs. A: Lymph node metastasis occurred in 100% of psiSCR- and psiVEGF-D-treated mice, while metastasis was reduced to 67% that of the control with psiVEGF-C treatment. B: The average number of metastatic lymph nodes per mouse was significantly lower in mice receiving psiVEGF-C, as compared to those receiving psiSCR. A tendency for decreased nodal involvement was seen in psiVEGF-D-treated mice, but this was not statistically significant. C: psiVEGF-C-treated mice also exhibited decreased incidence of lung metastasis, while treatment with psiVEGF-D had no effect. D: Development of larger metastatic lung nodules >250 µm was significantly reduced only in the psiVEGF-C-treated group. E: psiVEGF-C treatment appeared to reduce the total overall metastatic burden; Silencing Vegf-d had minimal effect. F: The average number of organs with metastases per mouse was significantly reduced only in the psiVEGF-C-treated group. Data represent the mean±SD. Number of animals examined was nine in the psiSCR-treated group, nine in the psiVEGF-C-treated group and ten in the psiVEGF-D-treated group. *$p<0.05$; **$p<0.01$ compared with the psiSCR-treated control.*

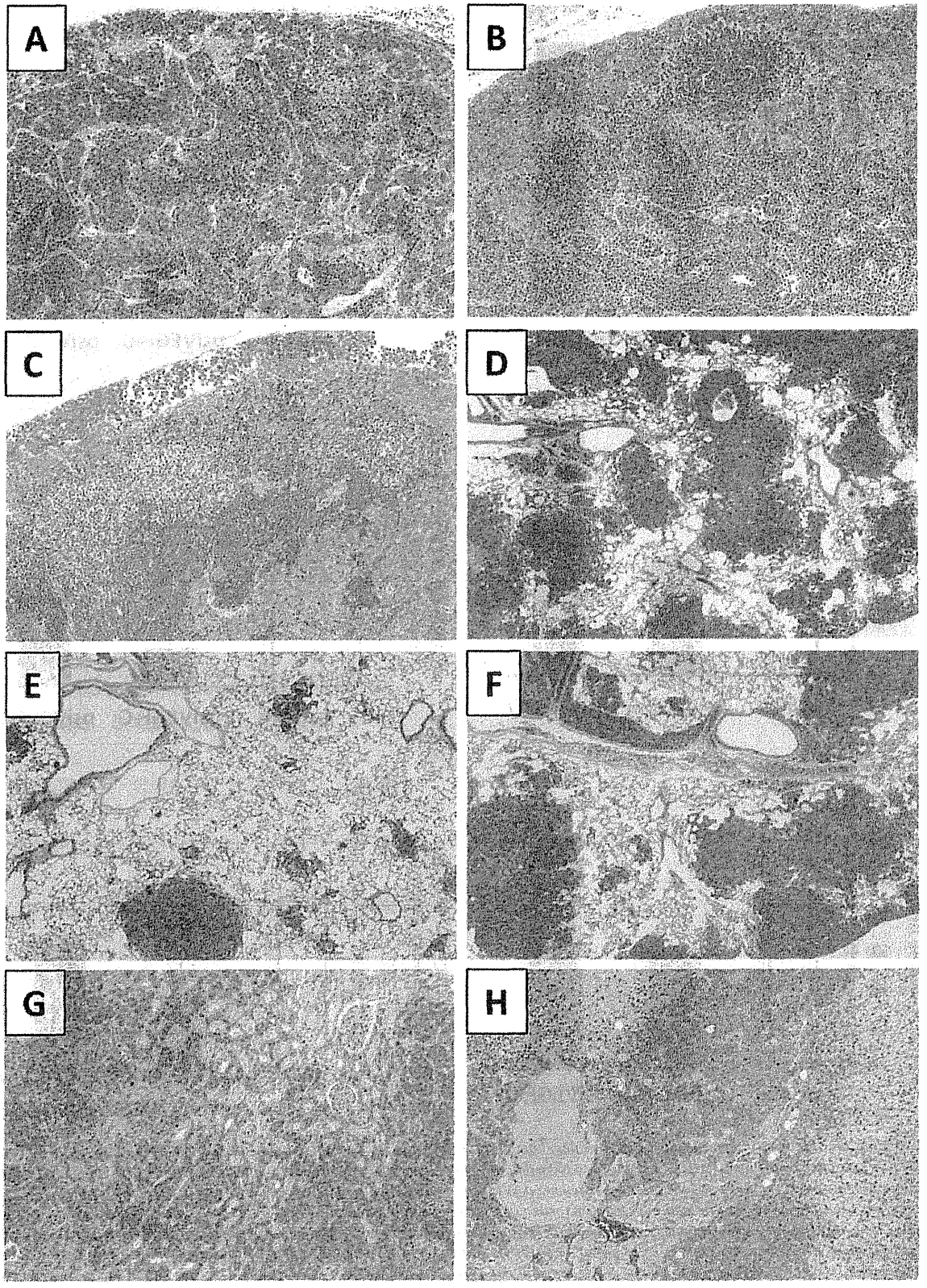

Figure 5. *Continued*

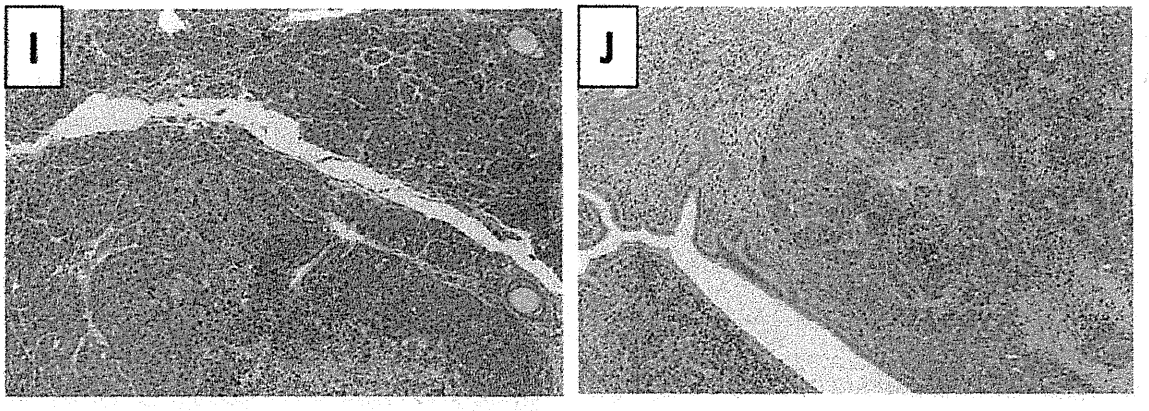

Figure 5. *Mammary tumor metastases as demonstrated by hematoxylin and eosin (H&E) histopathology. A: In a lymph node of a control mouse, metastatic carcinoma cells fill the sinusoidal space. B: Metastatic carcinoma cells are more localized to the subcapsular space in a lymph node from a mouse receiving psiVEGF-C. C: In a lymph node from a mouse receiving psiVEGF-D, metastatic carcinoma cells were observed in both the subcapsular and sinusoidal spaces. D: Metastatic foci in the lungs of a psiSCR-treated control mouse, showing many small-to-large foci and nodules. E: Metastatic lung lesions were much smaller in the lungs of mice treated with psiVEGF-C than in the control mice. F: Metastatic foci in the lungs of mice given psiVEGF-D were similar to those found in psiSCR mice in terms of number and size. G: Kidney metastasis in a control mouse receiving psiSCR. H: Metastasis to the adrenal of a control mouse. I: Ovarian metastasis in a mouse receiving psiVEGF-D. J: Uterine metastasis in a mouse receiving psiVEGF-C. A-C and G-J, original magnification ×100; D-F, original magnification ×40.*

psiVEGF-D-treated groups, but in only 67% of mice treated with psiVEGF-C (Figure 4A; Figure 5A-C); furthermore, treatment with psiVEGF-C caused a significant reduction in the average number of cancerous nodes per mouse (Figure 4B). Some insignificant reduction also occurred in the psiVEGF-D-treated group as compared to the psiSCR-treated group.

Metastasis to the lungs followed a similar pattern, as illustrated in Figures 4C-D and 5D-F. Lung metastasis developed in ~89% of mice in both the psiSCR- and psiVEGF-D-treated groups, while treatment with psiVEGF-C reduced the incidence to 44% (Figure 4C). This degree of reduction was not statistically significant. However, down-regulation of *Vegf-c* did significantly reduce the number of large (>250 μm) metastatic nodules (Figure 5E) as compared to the control (Figure 4D; Figure 5D and F).

Metastatic foci were also observed in kidneys, adrenals, ovaries and uterus (Figure 5G-J). With respect to bilateral organs, metastasis to the only unilateral organ was counted as one, and metastases to the bilateral organs were counted as two. The multiplicity of overall metastasis is presented in Figure 4E and F. The total number of organs affected per group tended to be much lower in mice treated with psiVEGF-C as compared to mice in both the control and the psiVEGF-D treatment groups (Figure 4E); similarly, the average number of all organs with metastasis per mouse was significantly lower in the psiVEGF-C-treated group as compared to the psiSCR-treated group (Figure 4F).

Lymphatic and blood microvessel density in treated mammary tumors. Intratumoral podoplanin-positive lymphatic microvessels are demonstrated in Figure 6A-C. Lymphatic vessels were well-developed in the outer, superficial layers of the mammary tumors in all groups, and tumor cells were frequently observed within the lumina of dilated vessels in both control (Figure 6A) and treated animals (Figure 6B and C). As shown in Figure 7A, significantly fewer vessels containing cancer cells were detected in psiVEGF-C-treated *vs.* psiSCR-treated tumors, suggesting suppression of lymphatic migration. Fewer vessels harboring migrating cells were also found in psiVEGF-D-treated *vs.* control tumors, but the difference was significant.

Blood microvessel density, as determined by immunohistochemical analysis for the blood vessel endothelial cell marker CD31 (Figure 6D-F), was significantly lower in the group given siRNA therapy targeting *Vegf-c* compared to the psiSCR-treated group (Figure 7B).

Discussion

As the presence and degree of metastasis is a significant prognostic indicator for survival in most types of cancer, anti-metastatic therapies are of paramount importance. Dissemination of cancer cells can occur in different ways *e.g.* local tissue invasion and/or migration *via* blood and lymphatic vessels. Malignant cells also move into the bloodstream to reach distant sites, and lymph/blood crossover occurs; lung metastasis may initially occur through the lymphatics, but cancer cells can influx into the thoracic duct, the left subclavian vein, through the right ventricle and settle into lung tissue. The most common pathway of initial dissemination of many solid malignancies is *via* the lymphatics, with varying

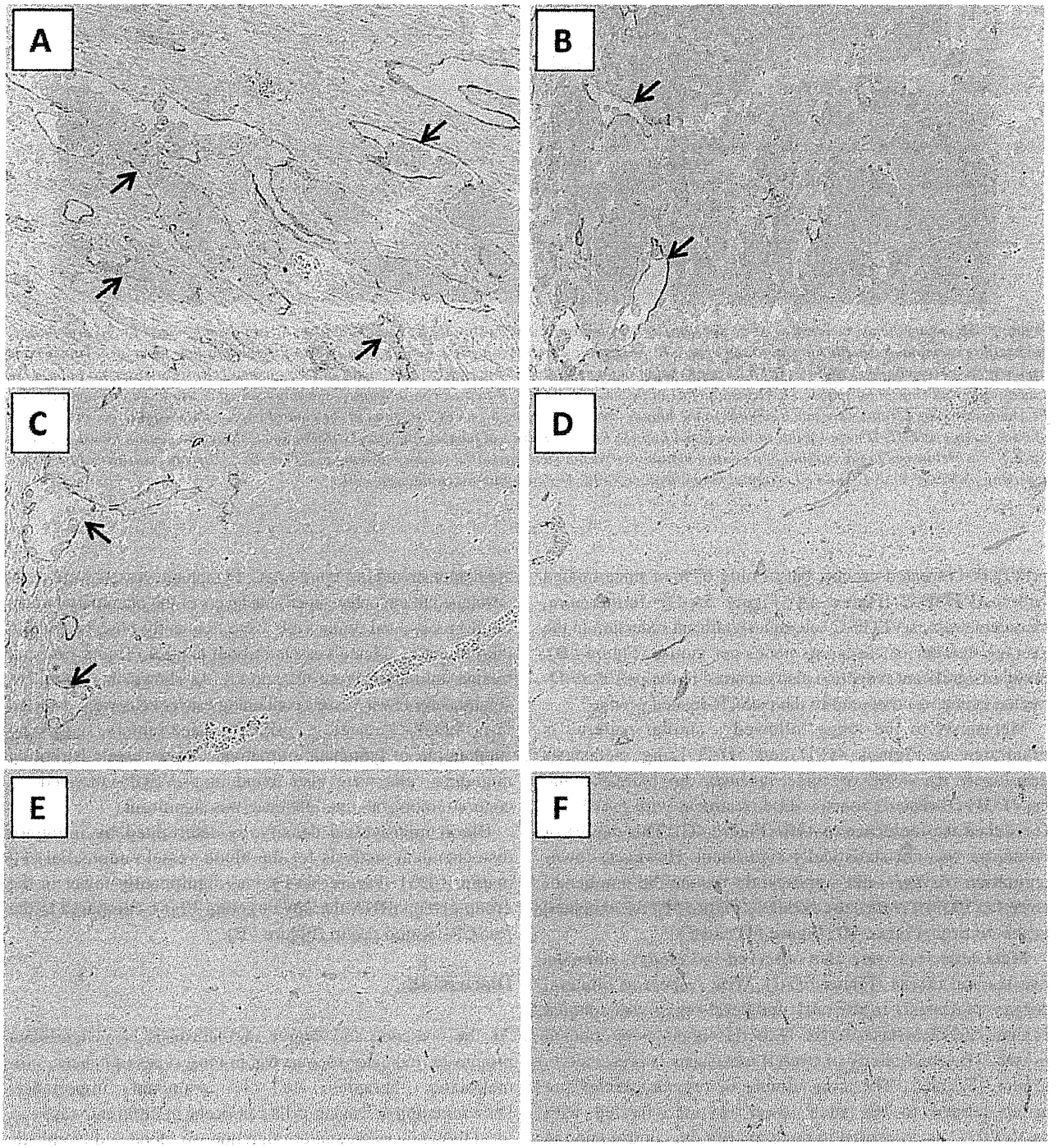

Figure 6. *Immunohistochemical (IHC) analysis of lymphangiogenesis and angiogenesis in mammary tumors transfected with psiSCR, psiVEGF-C, or psiVEGF-D. Lymphatic vessels were often dilated and frequently contained migrating tumor cells (arrows) within the lumina. A: Podoplanin-positive lymphatic endothelium in a control mouse with multiple intraluminal cells. B: Notice fewer dilated lymphatic vessels with migrating cancer cells in a mouse treated with psiVEGF-C. C: Intratumoral dilated lymphatic vessels of a mouse treated with psiVEGF-D. D: Representative section of a tumor transfected with psiSCR, showing a high density of well-developed and CD31-positive blood microvessels. E: CD31-positive blood microvessels tended to be fewer in tumors transfected with psiVEGF-C than with control or psiVEGF-D. F: Tumors treated with psiVEGF-D appeared similar to those in the psiSCR group. A-C: Anti-podoplanin IHC, original magnification ×200. D-F: anti-CD31 IHC, original magnification ×100.*

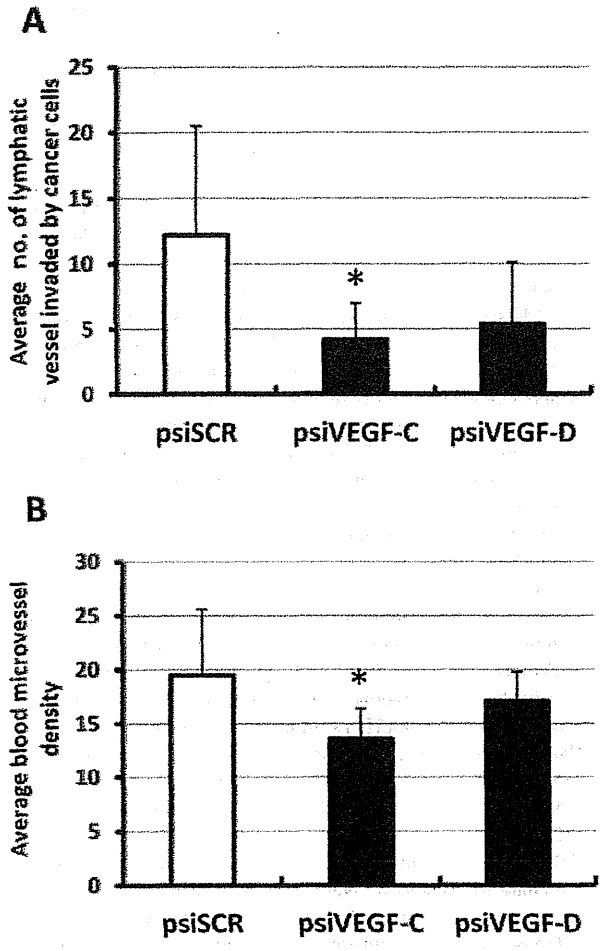

Figure 7. *Quantitative analysis of lymphatic cellular migration and blood microvessel density. A: Compared to the control, the average number of lymphatic vessels containing intraluminal cancer cells was lower in both psiVEGF-C and psiVEGF-D-treated mice, but the difference was only statistically significant with psiVEGF-C treatment. B: Blood microvessel density in psiVEGF-C-treated tumors was also significantly reduced vs. psiSCR-treated control. Data represent the mean±SD. *p<0.05 compared with the psiSCR-treated controls. In both vascular analyses, the number of examined animals was four or five in the psiSCR-treated group, nine in the psiVEGF-C-treated group and seven in the psiVEGF-D-treated group.*

patterns of spread *via* afferent ducts (32). Lymphatic and blood capillaries present in tumors and surrounding tissues provide migrating cells entrance to the system. Involvement of the nearby sentinel nodes precedes involvement of more distal nodes and subsequent seeding of distant organs.

Expression of VEGF-C and VEGF-D correlates with lymph node metastasis in a variety of human cancer types, including breast neoplasms (19, 33, 34), although, in contrast to VEGF-C, the role of VEGF-D is more equivocal. In at least one study, no association between VEGF-D and lymph node metastasis was found in human breast cancer (35), while another group of investigators linked high expression of VEGF-A and VEGF-C, but not VEGF-D, with poor prognosis (36). More recently, a clinical study demonstrated that only tumor-derived VEGF-C induced pre-metastatic sentinel node lymphangionenesis in primary breast cancer (37).

In many animal models of cancer, overexpression of both VEGF-C and VEGF-D evidently enhanced tumor lymphangiogenesis and nodal/distant organ metastasis (10-16), and siRNA down-regulation of VEGF-C reduced lymph node and lung metastases in murine mammary models (21, 38). An endogenous soluble isoform of the VEGF-C receptor, sVEGFR-2 was identified and shown to be a specific inhibitor of lymphatic vessel growth (39); a subsequent study showed sVEGFR-2 suppressed tumor growth and lymph node metastasis in a mouse mammary model specifically through inhibition of lymphangiogenesis (23). VEGFR-3, the co-receptor for both VEGF-C and VEGF-D, is predominantly expressed on lymphatic endothelial cells (40), and VEGF-C/D-dependent receptor activation stimulates both lymph endothelial cells and lymphatic vessel development (8, 9). Using soluble VEGFR-3 to sequester VEGF-C and VEGF-D effectively blocked VEGFR-3 signaling and inhibited lymphangiogenesis and lymph node metastasis in animal models (41-43), while an antibody to VEGF-D suppressed VEGF-D-induced lymphatic spread (14).

We attempted to refine *Vegf-c/d* down-regulation by first isolating the most effective silencing siRNA sequences and then directly treating highly metastatic mammary tumors *in vivo* with those sequences in a transfectable plasmid vector. Although intratumoral transfection with psiVEGF-C or psiVEGF-D reduced the average number of metastatic lymph nodes, statistically significant reduction was obtained only with psiVEGF-C transfection. Silencing *Vegf-c* also resulted in significant reductions in treated tumor volumes, in the average number of metastatic nodules of the lungs, and in the average number of other organs affected by metastasis. In contrast, siRNA therapy targeting *Vegf-d* gave equivocal results; it was ineffective in modulating overall organ metastasis, but did show some reduction of tumor volume increment, average number of lymph node metastases and average number of dilated lymphatic vessels with invading cancer cells. Carter *et al.* reported that once human breast carcinomas reach 4 cm or larger, the chance of tumor recurrence and metastasis increases dramatically (44). The reduction in tumor volume and size with psiVEGF-C could thus have clinical significance. A similar pattern emerged when analyzing blood microvessel density and lymphatic vessel invasion; transfection with psiVEGF-D tended to reduce both parameters, but psiVEGF-C treatment was significantly more effective. This was a much stronger anti-metastatic effect than we had previously obtained (21), due, we believe, to the selection and use of a more effective *Vegf-c* siRNA sequence.

In conclusion, treatment with psiVEGF-C, but not psiVEGF-D, significantly suppressed wide-spectrum organ metastasis and several parameters of tumor metastasis in a mouse model with prognostic significance in human cancer, suggesting a potential clinical therapeutic option in the treatment of human metastatic disease.

Acknowledgements

This investigation was supported by a Grant-in-Aid for Scientific Research (C)(2) from the Ministry of Education, Culture, Sports, Science and Technology (MEXT) of Japan (no. 17591360 to M.A. Shibata). We thank Ms. Naomi Nakano (Osaka Health Science University) and Ms. Akiko Yoshida (National Cerebral and Cardiovascular Center Research Institute) for their excellent secretarial assistance.

References

1 International Agency Research on Cancer. Globocan 2008. http://www-dep.iarc.fr/. (10 September 2013, date last accessed).

2 Agarwal G, Pradeep PV, Aggarwal V, Yip CH and Cheung PS: Spectrum of breast cancer in Asian women. World J Surg *31*: 1031-1040, 2007.

3 Brinton LA, Sherman ME, Carreon JD and Anderson WF: Recent trends in breast cancer among younger women in the United States. J Natl Cancer Inst *100*: 1643-1648, 2008.

4 Bouchardy C, Fioretta G, Verkooijen HM, Vlastos G, Schaefer P, Delaloye JF, Neyroud-Caspar I, Balmer Majno S, Wespi Y, Forni M, Chappuis P, Sappino AP and Rapiti E: Recent increase of breast cancer incidence among women under the age of forty. Br J Cancer *96*: 1743-1746, 2007.

5 Nguyen DX and Massague J: Genetic determinants of cancer metastasis. Nat Rev Genet *8*: 341-352, 2007.

6 Cody HS, 3rd, Borgen PI and Tan LK: Redefining prognosis in node-negative breast cancer: can sentinel lymph node biopsy raise the threshold for systemic adjuvant therapy? Ann Surg Oncol *11*: 227S-230S, 2004.

7 Achen MG and Stacker SA: Molecular control of lymphatic metastasis. Ann N Y Acad Sci *1131*: 225-234, 2008.

8 Joukov V, Pajusola K, Kaipainen A, Chilov D, Lahtinen I, Kukk E, Saksela O, Kalkkinen N and Alitalo K: A novel vascular endothelial growth factor, VEGF-C, is a ligand for the Flt4 (VEGFR-3) and KDR (VEGFR-2) receptor tyrosine kinases. EMBO J *15*: 290-298, 1996.

9 Achen MG, Jeltsch M, Kukk E, Makinen T, Vitali A, Wilks AF, Alitalo K and Stacker SA: Vascular endothelial growth factor D (VEGF-D) is a ligand for the tyrosine kinases VEGF receptor 2 (Flk1) and VEGF receptor 3 (Flt4). Proc Natl Acad Sci USA *95*: 548-553, 1998.

10 Skobe M, Hawighorst T, Jackson DG, Prevo R, Janes L, Velasco P, Riccardi L, Alitalo K, Claffey K and Detmar M: Induction of tumor lymphangiogenesis by VEGF-C promotes breast cancer metastasis. Nat Med *7*: 192-198, 2001.

11 Mandriota SJ, Jussila L, Jeltsch M, Compagni A, Baetens D, Prevo R, Banerji S, Huarte J, Montesano R, Jackson DG, Orci L, Alitalo K, Christofori G and Pepper MS: Vascular endothelial growth factor-C-mediated lymphangiogenesis promotes tumour metastasis. EMBO J *20*: 672-682, 2001.

12 Karpanen T, Egeblad M, Karkkainen MJ, Kubo H, Ylä-Herttuala S, Jaattela M and Alitalo K: Vascular endothelial growth factor C promotes tumor lymphangiogenesis and intralymphatic tumor growth. Cancer Res *61*: 1786-1790, 2001.

13 Achen MG, Mann GB and Stacker SA: Targeting lymphangiogenesis to prevent tumour metastasis. Br J Cancer *94*: 1355-1360, 2006.

14 Stacker SA, Caesar C, Baldwin ME, Thornton GE, Williams RA, Prevo R, Jackson DG, Nishikawa S, Kubo H and Achen MG: VEGF-D promotes the metastatic spread of tumor cells *via* the lymphatics. Nat Med *7*: 186-191, 2001.

15 Von Marschall Z, Scholz A, Stacker SA, Achen MG, Jackson DG, Alves F, Schirner M, Haberey M, Thierauch KH, Wiedenmann B and Rosewicz S: Vascular endothelial growth factor-D induces lymphangiogenesis and lymphatic metastasis in models of ductal pancreatic cancer. Int J Oncol *27*: 669-679, 2005.

16 Kopfstein L, Veikkola T, Djonov VG, Baeriswyl V, Schomber T, Strittmatter K, Stacker SA, Achen MG, Alitalo K and Christofori G: Distinct roles of vascular endothelial growth factor-D in lymphangiogenesis and metastasis. Am J Pathol *170*: 1348-1361, 2007.

17 Mylona E, Alexandrou P, Mpakali A, Giannopoulou I, Liapis G, Markaki S, Keramopoulos A and Nakopoulou L: Clinicopathological and prognostic significance of vascular endothelial growth factors (VEGF)-C and -D and VEGF receptor 3 in invasive breast carcinoma. Eur J Surg Oncol *33*: 294-300, 2007.

18 Nakamura Y, Yasuoka H, Tsujimoto M, Imabun S, Nakahara M, Nakao K, Nakamura M, Mori I and Kakudo K: Lymph vessel density correlates with nodal status, VEGF-C expression, and prognosis in breast cancer. Breast Cancer Res Treat *91*: 125-132, 2005.

19 Nakamura Y, Yasuoka H, Tsujimoto M, Yang Q, Imabun S, Nakahara M, Nakao K, Nakamura M, Mori I and Kakudo K: Prognostic significance of vascular endothelial growth factor D in breast carcinoma with long-term follow-up. Clin Cancer Res *9*: 716-721, 2003.

20 Zhao YC, Ni XJ, Li Y, Dai M, Yuan ZX, Zhu YY and Luo CY: Peritumoral lymphangiogenesis induced by vascular endothelial growth factor C and D promotes lymph node metastasis in breast cancer patients. World J Surg Oncol *10*: 165, 2012.

21 Shibata MA, Morimoto J, Shibata E and Otsuki Y: Combination therapy with short interfering RNA vectors against VEGF-C and VEGF-A suppresses lymph node and lung metastasis in a mouse immunocompetent mammary cancer model. Cancer Gene Ther *15*: 776-786, 2008.

22 Shibata MA, Morimoto J and Otsuki Y: Suppression of murine mammary carcinoma growth and metastasis by HSV*tk*/GCV gene therapy using *in vivo* electroporation. Cancer Gene Ther *9*: 16-27, 2002.

23 Shibata MA, Ambati J, Shibata E, Albuquerque RJ, Morimoto J, Ito Y and Otsuki Y: The endogenous soluble VEGF receptor-2 isoform suppresses lymph node metastasis in a mouse immunocompetent mammary cancer model. BMC Med *8*: 69, 2010.

24 Shibata MA, Iinuma M, Morimoto J, Kurose H, Akamatsu K, Okuno Y, Akao Y and Otsuki Y: α-Mangostin extracted from the pericarp of the mangosteen (*Garcinia mangostana* Linn) reduces tumor growth and lymph node metastasis in an immunocompetent xenograft model of metastatic mammary cancer carrying a p53 mutation. BMC Med *9*: 69, 2011.

25 Shibata MA, Shibata E, Morimoto J, Eid NAS, Tanaka Y, Watanabe M and Otsuki Y: An immunocompetent murine model of metastatic mammary cancer accessible to bioluminescence imaging. Anticancer Res *29*: 4389-4396, 2009.
26 Livak KJ and Schmittgen TD: Analysis of relative gene expression data using real-time quantitative PCR and the 2(-Delta Delta C(T)) Method. Methods *25*: 402-408, 2001.
27 Shibata MA, Miwa Y, Miyashita M, Morimoto J, Abe H and Otsuki Y: Electrogene transfer of an Epstein-Barr virus-based plasmid replicon vector containing the diphtheria toxin A gene suppresses mammary carcinoma growth in SCID mice. Cancer Sci *96*: 434-440, 2005.
28 Shibata MA, Ito Y, Morimoto J, Kusakabe K, Yoshinaka R and Otsuki Y: In vivo electrogene transfer of interleukin-12 inhibits tumor growth and lymph node and lung metastases in mouse mammary carcinomas. J Gene Med *8*: 335-352, 2006.
29 Shibata MA, Morimoto J, Doi H, Morishima S, Naka M and Otsuki Y: Electrogene therapy using endostatin, with or without suicide gene therapy, suppresses murine mammary tumor growth and metastasis. Cancer Gene Ther *14*: 268-278, 2007.
30 Shibata MA, Liu M-L, Knudson MC, Shibata E, Yoshidome K, Bandy T, Korsmeyer SJ and Green JE: Haploid loss of *bax* leads to accelerated mammary tumor development in C3(1)/SV40-TAg transgenic mice: reduction in protective apoptotic response at the preneoplastic stage. EMBO J *18*: 2692-2701, 1999.
31 Gorrin-Rivas MJ, Arii S, Furutani M, Mizumoto M, Mori A, Hanaki K, Maeda M, Furuyama H, Kondo Y and Imamura M: Mouse macrophage metalloelastase gene transfer into a murine melanoma suppresses primary tumor growth by halting angiogenesis. Clin Cancer Res *6*: 1647-1654, 2000.
32 Sleeman JP: The lymph node as a bridgehead in the metastatic dissemination of tumors. Recent Results Cancer Res *157*: 55-81, 2000.
33 Salven P, Lymboussaki A, Heikkila P, Jaaskela-Saari H, Enholm B, Aase K, von Euler G, Eriksson U, Alitalo K and Joensuu H: Vascular endothelial growth factors VEGF-B and VEGF-C are expressed in human tumors. Am J Pathol *153*: 103-108, 1998.
34 Valtola R, Salven P, Heikkila P, Taipale J, Joensuu H, Rehn M, Pihlajaniemi T, Weich H, deWaal R and Alitalo K: VEGFR-3 and its ligand VEGF-C are associated with angiogenesis in breast cancer. Am J Pathol *154*: 1381-1390, 1999.
35 Currie MJ, Hanrahan V, Gunningham SP, Morrin HR, Frampton C, Han C, Robinson BA and Fox SB: Expression of vascular endothelial growth factor D is associated with hypoxia inducible factor (HIF-1α) and the HIF-1α target gene DEC1, but not lymph node metastasis in primary human breast carcinomas. J Clin Pathol *57*: 829-834, 2004.
36 Mohammed RA, Green A, El-Shikh S, Paish EC, Ellis IO and Martin SG: Prognostic significance of vascular endothelial cell growth factors -A, -C and -D in breast cancer and their relationship with angio- and lymphangiogenesis. Br J Cancer *96*: 1092-1100, 2007.
37 Zhao YC, Ni XJ, Wang MH, Zha XM, Zhao Y and Wang S: Tumor-derived VEGF-C, but not VEGF-D, promotes sentinel lymph node lymphangiogenesis prior to metastasis in breast cancer patients. Med Oncol *29*: 2594-2600, 2012.
38 Chen Z, Varney ML, Backora MW, Cowan K, Solheim JC, Talmadge JE and Singh RK: Down-regulation of vascular endothelial cell growth factor-C expression using small interfering RNA vectors in mammary tumors inhibits tumor lymphangiogenesis and spontaneous metastasis and enhances survival. Cancer Res *65*: 9004-9011, 2005.
39 Albuquerque RJ, Hayashi T, Cho WG, Kleinman ME, Dridi S, Takeda A, Baffi JZ, Yamada K, Kaneko H, Green MG, Chappell J, Wilting J, Weich HA, Yamagami S, Amano S, Mizuki N, Alexander JS, Peterson ML, Brekken RA, Hirashima M, Capoor S, Usui T, Ambati BK and Ambati J: Alternatively spliced vascular endothelial growth factor receptor-2 is an essential endogenous inhibitor of lymphatic vessel growth. Nat Med *15*: 1023-1030, 2009.
40 Kaipainen A, Korhonen J, Mustonen T, van Hinsbergh VW, Fang GH, Dumont D, Breitman M and Alitalo K: Expression of the fms-like tyrosine kinase 4 gene becomes restricted to lymphatic endothelium during development. Proc Natl Acad Sci USA *92*: 3566-3570, 1995.
41 He Y, Kozaki K, Karpanen T, Koshikawa K, Yla-Herttuala S, Takahashi T and Alitalo K: Suppression of tumor lymphangiogenesis and lymph node metastasis by blocking vascular endothelial growth factor receptor 3 signaling. J Natl Cancer Inst *94*: 819-825, 2002.
42 Shimizu K, Kubo H, Yamaguchi K, Kawashima K, Ueda Y, Matsuo K, Awane M, Shimahara Y, Takabayashi A, Yamaoka Y and Satoh S: Suppression of VEGFR-3 signaling inhibits lymph node metastasis in gastric cancer. Cancer Sci *95*: 328-333, 2004.
43 Lin J, Lalani AS, Harding TC, Gonzalez M, Wu WW, Luan B, Tu GH, Koprivnikar K, VanRoey MJ, He Y, Alitalo K and Jooss K: Inhibition of lymphogenous metastasis using adeno-associated virus-mediated gene transfer of a soluble VEGFR-3 decoy receptor. Cancer Res *65*: 6901-6909, 2005.
44 Carter CL, Allen C and Henson DE: Relation of tumor size, lymph node status, and survival in 24,740 breast cancer cases. Cancer *63*: 181-187, 1989.

Received July 26, 2013
Revised September 11, 2013
Accepted September 12, 2013

Instructions to Authors 2013

General Policy. ANTICANCER RESEARCH (AR) will accept original high quality works and reviews on all aspects of experimental and clinical cancer research. The Editorial Policy suggests that priority will be given to papers advancing the understanding of cancer causation, and to papers applying the results of basic research to cancer diagnosis, prognosis, and therapy. AR will also accept the following for publication: (a) Abstracts and Proceedings of scientific meetings on cancer, following consideration and approval by the Editorial Board; (b) Announcements of meetings related to cancer research; (c) Short reviews (of approximately 120 words) and announcements of newly received books and journals related to cancer, and (d) Announcements of awards and prizes.

The principal aim of AR is to provide prompt publication (print and online) for original works of high quality, generally within 1-2 months from final acceptance. Manuscripts will be accepted on the understanding that they report original unpublished works on the cancer problem that are not under consideration for publication by another journal, and that they will not be published again in the same form. All authors should sign a submission letter confirming the approval of their article contents. All material submitted to AR will be subject to review, when appropriate, by two members of the Editorial Board and by one suitable outside referee. The Editors reserve the right to improve manuscripts on grammar and style.

The Editors and Publishers of AR accept no responsibility for the contents and opinions expressed by the contributors. Authors should warrantee due diligence in the creation and issuance of their work.

NIH Open Access Policy. The journal acknowledges that authors of NIH funded research retain the right to provide a copy of the final manuscript to the NIH four months after publication in ANTICANCER RESEARCH, for public archiving in PubMed Central.

Copyright. Once a manuscript has been published in ANTICANCER RESEARCH, which is a copyrighted publication, the legal ownership of all published parts of the paper has been transferred from the Author(s) to the journal. Material published in the journal may not be reproduced or published elsewhere without the written consent of the Managing Editor or Publisher.

Format. Two types of papers may be submitted: (i) Full papers containing completed original work, and (ii) review articles concerning fields of recognisable progress. Papers should contain all essential data in order to make the presentation clear. Reasonable economy should be exercised with respect to the number of tables and illustrations used. Papers should be written in clear, concise English. Spelling should follow that given in the "Shorter Oxford English Dictionary".

Manuscripts. Submitted manuscripts should not exceed fourteen (14) pages (approximately 250 words per double - spaced typed page), including abstract, text, tables, figures, and references (corresponding to 4 printed pages). Papers exceeding four printed pages will be subject to excess page charges. All manuscripts should be divided into the following sections:
(a) *First page* including the title of the presented work [not exceeding fifteen (15) words], full names and full postal addresses of all Authors, name of the Author to whom proofs are to be sent, key words, an abbreviated running title, an indication "review", "clinical", "epidemiological", or "experimental" study, and the date of submission. (Note: The order of the Authors is not necessarily indicative of their contribution to the work. Authors may note their individual contribution(s) in the appropriate section(s) of the presented work); (b) *Abstract* not exceeding 150 words, organized according to the following headings: Background/Aim - Materials and Methods/Patients and Methods - Results - Conclusion; (c) *Introduction;* (d) *Materials and Methods/Patients and Methods;* (e) *Results;* (f) *Discussion;* (g) *Acknowledgements;* (h) *References*. All pages must be numbered consecutively. Footnotes should be avoided. Review articles may follow a different style according to the subject matter and the Author's opinion. Review articles should not exceed 35 pages (approximately 250 words per double-spaced typed page) including all tables, figures, and references.

Figures. All figures (whether photographs or graphs) should be clear, high contrast, at the size they are to appear in the journal: 8.00 cm (3.15 in.) wide for a single column; 17.00 cm (6.70 in.) for a double column; maximum height: 20.00 cm (7.87 in.). Graphs must be submitted as photographs made from drawings and must not require any artwork, typesetting, or size modifications. Symbols, numbering and lettering should be clearly legible. The number and top of each figure must be indicated. Colour plates are charged.

Tables. Tables should be typed double-spaced on a separate page, numbered with Roman numerals and should include a short title.

References. Authors must assume responsibility for the accuracy of the references used. Citations for the reference sections of submitted works should follow the standard form of "Index Medicus" and must be numbered consecutively. In the text, references should be cited by number. Examples: 1 Sumner AT: The nature of chromosome bands and their significance for cancer research. Anticancer Res 1: 205-216, 1981. 2 McGuire WL and Chamnes GC: Studies on the oestrogen receptor in breast cancer. In: Receptors for Reproductive Hormones (O' Malley BW, Chamnes GC (eds.). New York, Plenum Publ Corp., pp 113-136, 1973.

Nomenclature and Abbreviations. Nomenclature should follow that given in "Chemical Abstracts", "Index Medicus", "Merck Index", "IUPAC –IUB", "Bergey's Manual of Determinative Bacteriology", The CBE Manual for Authors, Editors and Publishers (6th edition, 1994), and MIAME Standard for Microarray Data. Human gene symbols may be obtained from the HUGO Gene Nomenclature Committee (HGNC) (http://www.gene.ucl.ac.uk/). Approved mouse nomenclature may be obtained from http://www.informatics.jax.org/. Standard abbreviations are preferable. If a new abbreviation is used, it must be defined on first usage.

Clinical Trials. Authors of manuscripts describing clinical trials should provide the appropriate clinical trial number in the correct format in the text.

For International Standard Randomised Controlled Trials (ISRCTN) Registry (a not-for-profit organization whose registry is administered by Current Controlled Trials Ltd.) the unique number must be provided in this format: ISRCTNXXXXXXXX (where XXXXXXXX represents the unique number, always prefixed by "ISRCTN"). Please note that there is no space between the prefix "ISRCTN" and the number. Example: ISRCTN47956475.

For Clinicaltrials.gov registered trials, the unique number must be provided in this format: NCTXXXXXXXX (where XXXXXXXX represents the unique number, always prefixed by 'NCT'). Please note that there is no space between the prefix 'NCT' and the number. Example: NCT00001789.

Ethical Policies and Standards. ANTICANCER RESEARCH agrees with and follows the "Uniform Requirements for Manuscripts Submitted to Biomedical Journals" established by the International Committee of Medical Journal Editors in 1978 and updated in October 2001 (www.icmje.org). Microarray data analysis should comply with the "Minimum Information About Microarray Experiments (MIAME) standard". Specific guidelines are provided at the "Microarray Gene Expression Data Society" (MGED) website. Presentation of genome sequences should follow the guidelines of the NHGRI Policy on Release of Human Genomic Sequence Data. Research involving human beings must adhere to the principles of the Declaration of Helsinki and Title 45, U.S. Code of Federal Regulations, Part 46, Protection of Human Subjects, effective December 13, 2001. Research involving animals must adhere to the Guiding Principles in the Care and Use of Animals approved by the Council of the American Physiological Society. The use of animals in biomedical research should be under the careful supervision of a person adequately trained in this field and the animals must be treated humanely at all times. Research involving the use of human foetuses, foetal tissue, embryos and embryonic cells should adhere to the U.S. Public Law 103-41, effective December 13, 2001.

Submission of Manuscripts. Please follow the Instructions to Authors regarding the format of your manuscript and references. There are 3 ways to submit your article (NOTE: Please use only one of the 3 options. Do not send your article twice.):

1. To submit your article online please visit: IIAR-Submissions (http://www.iiar-anticancer.org/submissions/login.php)
2. You can send your article via e-mail to journals@iiar-anticancer.org. Please remember to always indicate the name of the journal you wish to submit your paper. The text should be sent as a Word document (*doc) attachment. Tables, figures and cover letter can also be sent as e-mail attachments.
3. You can send the manuscript of your article via regular mail in a USB stick, DVD, CD or floppy disk (including text, tables and figures) together with three hard copies to the following address:
   John G. Delinasios
   International Institute of Anticancer Research (IIAR)
   Editorial Office of ANTICANCER RESEARCH,
   IN VIVO, CANCER GENOMICS and PROTEOMICS.
   1st km Kapandritiou-Kalamou Road
   P.O. Box 22, GR-19014 Kapandriti, Attiki
   GREECE

Submitted articles will not be returned to Authors upon rejection.

Galley Proofs. Unless otherwise indicated, galley proofs will be sent to the first-named Author of the submission. Corrections of galley proofs should be limited to typographical errors. Reprints, PDF files, and/or Open Access may be ordered after the acceptance of the paper. Requests should be addressed to the Editorial Office.

Increase in Secretory Sphingomyelinase Activity and Specific Ceramides in the Aorta of Apolipoprotein E Knockout Mice during Aging

Keiko Kobayashi,*[a] Eri Nagata,[a] Kazuki Sasaki,[a] Mariko Harada-Shiba,[b] Shosuke Kojo,*[c] and Hiroe Kikuzaki[a]

[a] *Department of Food Science and Nutrition, Nara Women's University; Nara 630–8506, Japan:* [b] *Department of Molecular Innovation in Lipidology, National Cerebral and Cardiovascular Center Research Institute; Suita, Osaka 565–8565, Japan: and* [c] *The Open University of Japan; Wakaba, Mihama, Chiba 261–8586, Japan.*
Received March 2, 2013; accepted May 12, 2013

Atherosclerosis is caused by many factors, one of which is oxidative stress. We recently demonstrated that systemic oxidative stress increased secretory sphingomyelinase (sSMase) activity and generated ceramides in the plasma of diabetic rats. In addition, we also showed that the total ceramide level in human plasma correlated with the level of oxidized low-density lipoprotein. To investigate the relationship between ceramide species and atherogenesis during aging, we compared age-related changes in ceramide metabolism in apolipoprotein E knock out mice (apoE$^{-/-}$) and wild type mice (WT). Although the total plasma ceramide level was higher in apoE$^{-/-}$ than that in WT at all ages, it decreased with increasing age. sSMase activity increased at 65 weeks (w) of age in both strains of mice. When apoE$^{-/-}$ developed atherosclerosis at 15 w of age, C18:0, C22:0, and C24:0 ceramide levels in the apoE$^{-/-}$ aorta significantly increased. Furthermore, at 65 w of age C16:0 and C24:1 ceramide levels were significantly higher than those in WT. These results suggested that elevation in levels of specific ceramide species due to sSMase activity contributed to atherogenesis during aging.

Key words aging; apolipoprotein E; atherosclerosis; ceramide; sphingomyelinase

Cardiovascular disease is associated with aging. Hyperlipidemia and long-term exposure to various stimuli such as oxidative stress lead to atherosclerosis. Despite several indications that aging causes atherosclerosis, a specific factor associated with atherosclerosis that increases or decreases with aging is yet to be entirely identified. One possible factor is elevation of bioactive lipid such as ceramide. Ceramide regulates cell cycle arrest, apoptosis, and cellular senescence,[1] and serves as an intracellular second messenger in these processes.[2] Oxidative stress inducers such as UV light, antineoplastic drugs, and radiation stimulate ceramide accumulation in the cell.[3–6] Ceramide belongs to the sphingolipid family and comprises a saturated or unsaturated fatty acid of C16–C26 chain length bound to the amino group of sphingosine.

Ceramide is generated by *de novo* synthetic pathway as well as from the hydrolysis of sphingomyelin (SM) by sphingomyelinase (SMase). Sphingomyelinases are classified into five types on the basis of their optimum pH, subcellular localization, and cation dependence.[5,7] Among these enzymes acid SMase (aSMase) (optimal pH=4.8) operates in the endosomal/lysosomal compartment or plasma membrane.[8] Of note, the aSMase gene (*smpdl*) gives rise to two different enzymes lysosomal SMase *i.e.*, aSMase, and secretory SMase (sSMase) *via* alternative trafficking of the same protein precusor.[9,10] The vascular endothelium and macrophages secrete sSMase, which is the only enzyme responsible for sphingolytic activity in plasma.[11]

Elevated ceramide levels were recently shown to correlate with atherogenetic processes such as low-density lipoprotein (LDL) aggregation,[12] and form cell migration.[13] In relation to atherogenesis, we previously reported that the ceramide level in human plasma was positively correlated with both total cholesterol and oxidized apolipoprotein B-100 (oxLDL) levels.[14] Deevska *et al.*[15] reported that LDL-SM content and sSMase activity in LDL receptor knockout mice, which were fed an atherogenic diet, were increased. Excessive cholesterol intake increased plasma ceramides in apolipoprotein E knockout mice (apoE$^{-/-}$), a typical animal model for atherosclerosis.[16] In addition, we previously reported that the increase in plasma ceramide level was caused by increased activity of sSMase in the streptozotocin-induced diabetic rats,[17] thus suggesting that the elevation of plasma ceramide was an important factor in atherogenesis. sSMase activity also increased in response to stimulation of macrophages obtained from patients with chronic heart failure[18] and type 2 diabetes.[19] These studies indicated that oxidative stress resulted in ceramide accumulation by increasing sSMase activity.

To investigate the effect of aging on ceramide metabolism, we compared changes in tissue ceramides and related enzymes in apoE$^{-/-}$ with wild-type mice (WT), particularly focusing on SMase activity, which increased because of oxidative stress.[17,20,21]

MATERIALS AND METHODS

Materials All the solvents were purchased from Wako Pure Chemical Industries, Ltd. (Osaka, Japan). All other reagents were obtained from Nacalai Tesque Inc. (Kyoto, Japan). Authentic ceramides were purchased from Avanti Polar Lipids Inc. (Alabaster, AL, U.S.A.). Nitrobenzofurazan (NBD) C_6-SM was purchased from Molecular Probes Inc. (Eugene, OR, U.S.A.).

Animals This study was approved by the Animal Care Committee of Nara Women's University. Female WT (SLC: C57BL/6J; 4 or 13 weeks of age) were obtained from Japan SLC Co. (Hamamatsu, Shizuoka, Japan). Female apoE$^{-/-}$ were obtained from the Jackson Laboratory. The animals were housed in a room maintained at 24±2°C, with a 12h/12h

The authors declare no conflict of interest.

* To whom correspondence should be addressed. e-mail: keiko.kobayashi@cc.nara-wu.ac.jp; kojo@ouj.ac.jp

light/dark cycle. Animals were fed commercial laboratory chow (CE-2, Oriental Yeast Co., Osaka, Japan) and water *ad libitum*. Mice were sacrificed at the age of 7, 15, and 65 weeks (w) of age.

Analytical Methods Mice were anesthetized with Nembutal, and blood samples were collected by left ventricular puncture using a syringe containing sodium heparin as an anticoagulant. After perfusion with saline, the liver and aorta were dissected out. Plasma was separated from whole blood sample by centrifugation.

SMase Activity Assay SMase activities were measured using NBD C_6-SM as a substrate, and the assay was principally performed based on previous studies.[17,22] For sSMase analysis, a 800 μL assay mixture consisted of 15 μL of plasma and 785 μL of an assay buffer (0.1 mM $ZnSO_4$, 1 nmol NBD C_6-SM, 0.1% NP-40/62, 0.1 M sodium acetate buffer at pH 5.0) was incubated for 2 h at 37°C. The reaction was stopped by adding 1 mL of methanol. For aortic aSMase, which depended on zinc ion, the aorta was dissected and cleaned of visible fat debris. The tissue was homogenized on ice in 400 μL of phosphate buffered saline (10 mM, pH 7.4). Protein concentrations were determined according to the method of Lowry *et al.*[23] Aortic aSMase activity was determined by suspending the homogenate (1–2 mg protein/mL) in 800 μL assay mixture comprising of 0.1 mM $ZnSO_4$, 1 nmol NBD C_6-SM, 0.1% NP-40/62, and 0.1 M sodium acetate (pH 5.0). The reaction was continued for 2 h at 37°C and stopped by the addition of 2 mL methanol. NBD C_6-SM and generated NBD C_6-Ceramide were subsequently extracted according to the method of Bligh and Dyer.[24] The extract was dissolved in 0.5 mL methanol and analyzed using HPLC as described below. The samples (20 μL) were directly analyzed by HPLC with a Nova Pak 4 μm C18 column (3.9×150 mm, Waters Corporation, Milford, MA, U.S.A.). Elution was performed at a flow rate of 1 mL/min with a mixture of water, acetonitrile, and phosphoric acid at a volume ratio of 35 : 65 : 0.2. NBD fluorescence was determined using a fluorescence detector (Shimadzu, RF-10AXL, excitation at 466 nm and emission at 536 nm).

Data were expressed as mean±S.E.M., and analyzed by multiple comparison tests using Statcel software (OMS Publishing Inc., Tokyo, Japan). Using the Tukey–Kramer Procedure, the differences between group means were significant at $p<0.05$.

Ceramide Measurement Lipids were extracted according to the method of Folch *et al.*[25] Lipids were dissolved in chloroform and subjected to chromatography on Silica gel 60 thin-layer chromatography (TLC) plates (Merck, Darmstradt, Germany). Separation was performed using silica gel 60 TLC plates (Merck, Germany) as previous studies.[6,26] In brief, the first elution was made with a mixture of *n*-butanol–acetic acid–water (30 : 10 : 10, v/v/v) to the one third of the plate and the second elution was made to the top of the plate with a mixture of diethyl ether–*n*-hexane–acetic acid (90 : 10 : 1, v/v/v). The ceramide spot was visualized under the UV by staining with primulin spray. The ceramide spot was scratched from the TLC plates and collected into a glass tube. Extraction was made with 2 mL of a mixture of H_2O–CH_3OH–$CHCl_3$ (20 : 30 : 50, v/v/v) under shaking for 30 min. After centrifugation, the lower layer was collected. To the upper phase was added 1.5 mL of $CHCl_3$, and extraction was made an additional two times. The collected $CHCl_3$ solution was evaporated and resuspended in a mixture of 10 mL (liver) or 2 mL (aorta and plasma) of $CHCl_3$–CH_3OH (1 : 9, v/v). Standards and tissue ceramide extracts were stored at −20°C. The quantities of major ceramide species were measured by LC-MS/MS using a triple-quadrupole mass spectrometer [the ACQUITY TQD mass spectrometer (Waters Corporation, Milford, MA, U.S.A.)] equipped with the ACQUITY ultra performance liquid chromatography (UPLC) system (Waters Corporation, Milford, MA, U.S.A.). The ceramide species were separated using a column, [ACQUITY UPLC BEH, 1.7 μm, 2.1×50 mm, C18 (Waters Corporation, Milford, MA, U.S.A.)] at 50°C. UPLC gradient elution was applied beginning with 15% of mobile phase A (water containing 0.2% formic acid and 5 mM ammonium acetate) and 85% of mobile phase B (methanol containing 0.2% formic acid and 5 mM ammonium acetate) at a flow rate of 0.4 mL/min. The initial solvent condition was maintained for 3 min, and the percentage of the B solution was gradually increased with a linear gradient to 99% for 6 min. The column was equilibrated for 4 min with 85% mobile phase B prior to next injection. The total run time per injection was 13 min. The mass spectrometry settings were as follows: electrospray ionization (ESI) positive ion mode, capillary voltage, 3.0 kV; cone voltage, 20 V; source temperature, 120°C; and desolvation temperature, 350°C. The flow rates of nitrogen gas in the cone and desolvation gas were 50 and 600 L/h, respectively. Argon gas was used for collision-induced dissociation and maintenance of collision cell pressure at 10^{-4} mbar. Results were analyzed using multiple reaction monitoring (MRM). Mass spectra (*m/z*) for an internal standard (IS) and six major ceramides were set up at 426.4→264.2 for C8:0 ceramide (IS), and 538.4→264.2, 566.5→264.2, 622.5→264.3, 650.6→264.3, 648.6→264.3, 646.6→264.3 for C16:0, C18:0, C22:0, C24:0, C24:1, and C24:2 ceramides, respectively. Data acquisition was carried out by MassLynx software (version 4.1, Waters Corporation). Ceramide species were quantified using standard curves and ratios of the integrated peak areas of each ceramide species and C8:0 ceramide, which was used as an internal standard for quantification of the other ceramide species. Total ceramide content was calculated by addition of the amount of C16:0, C18:0, C22:0, C24:0, C24:1, and C24:2 ceramides. Data were expressed as an mean±S.E.M.

RESULTS

Change in SMase Activity Plasma sSMase activity was significantly elevated at 65 w of age in both apoE$^{-/-}$ and WT compared with level observed at 7 w of age (Table 1). At 7 w

Table 1. Changes in sSMase Activity in Plasma (pmol/mL/min) and Aortic aSMase Activity (pmol/mg protein/min) of Wild-Type and ApoE$^{-/-}$ Mice

	7 w WT	15 w WT	65 w WT	7 w apoE$^{-/-}$	15 w apoE$^{-/-}$	65 w apoE$^{-/-}$
sSMase	1599.6±171.6^{ab}	1666.7±83.6^{ab}	2688.7±175.1^{c}	657.3±86.9^{d}	1187.2± 121.7^{ad}	1990.2±207.1^{b}
Aortic aSMase	79.2±9.4^{a}	130.8±12.5^{bc}	271.5±14.3^{d}	113.8±13.5^{ab}	167.1±8.3^{c}	66.4±5.0^{a}

Values are presented as mean±S.E.M. for 4 or 5 animals in each group. Different superscript letters indicate significant differences at $p<0.05$ (Tukey–Kramer *post hoc* test).

of age, plasma sSMase activity was lower in apoE$^{-/-}$ than that in WT.

Aortic aSMase activity in WT was significantly elevated at 15 w of age compared with the level observed at 7w of age, the level increased further at 65w of age (Table 1). In contrast, aortic aSMase activity in apoE$^{-/-}$ was unchanged at 15w of age compared with that at 7w of age and declined significantly at 65w of age. Liver aSMase and neutral SMase activities were unchanged during aging in both apoE$^{-/-}$ and WT (data not shown).

Changes in Tissue Ceramide Levels The total aortic ceramide level in WT at 65w of age increased significantly compared with that observed at 7w of age (2.6-fold increase) (Table 2A). In the apoE$^{-/-}$ aorta, the total ceramide level was increased at 15w and 65w of age compared with the level observed at 7w of age (2.0, 1.9-fold, respectively). The total aortic ceramide concentration of apoE$^{-/-}$ was similar to that of WT at 7w of age (Table 2A); however, it was significantly higher than that of WT (2.7-fold) at 15w of age. Table 2A demonstrates the six major ceramide levels. In the WT aorta, C24:0, C24:1, and C24:2 ceramide levels at 65w of age were significantly higher than those at 7w of age (2.6, 2.9, 6.0-fold, respectively). In contrast, C18:0, C22:0, and C24:0 ceramide levels in apoE$^{-/-}$ aorta increased at 15 w of age compared with those observed at 7 w of age (2.7, 2.4, 2.2-fold, respectively). The C16:0, C24:1, and C24:2 ceramide levels in apoE$^{-/-}$ aorta at 65w of age increased compared with those at 7w of age (2.5, 2.3, 2.6-fold, respectively) (Table 2A).

Although the levels of almost all ceramide species changed in a similar manner to the total level, some ceramides showed a different behavior (Table 2A). The levels of C16:0, C18:0, C22:0, and C24:0 ceramides in the apoE$^{-/-}$ aorta were significantly higher than those of WT (2.4, 4.1, 3.5, 3.5-fold, respectively) at 15w of age.

The total plasma ceramide level in apoE$^{-/-}$ was significantly higher (4.4–5.9-fold) than that observed in WT at all ages

Table 2A. Levels of Ceramides in the Aorta of Wild-Type and ApoE$^{-/-}$ Mice

(A) Aorta ceramide levels (nmol/mg protein)

Aorta	7w WT	15w WT	65w WT	7w apoE$^{-/-}$	15w apoE$^{-/-}$	65w apoE$^{-/-}$
C16:0	1.08±0.18^{a}	1.53±0.15^{a}	2.48±0.32^{ac}	2.03±0.46^{ac}	3.70±0.52^{bc}	4.98±0.53^{b}
C18:0	0.38±0.04^{a}	0.38±0.03^{a}	0.74±0.07^{a}	0.58±0.14^{a}	1.53±0.14^{b}	0.47±0.04^{a}
C22:0	0.45 ± 0.06^{ab}	0.44 ± 0.05^{b}	0.95 ± 0.13^{a}	0.66 ± 0.14^{ab}	1.56 ± 0.18^{bc}	0.94 ± 0.08 ^{a}
C24:0	1.36±0.21^{ac}	1.33±0.10^{a}	3.52±0.46^{bd}	2.10±0.39^{ad}	4.69±0.55^{b}	3.03±0.29^{cd}
C24:1	0.58±0.12^{a}	1.03±0.12^{ab}	1.70±0.15^{b}	1.22±0.24^{ab}	1.79±0.25^{b}	2.82±0.31^{c}
C24:2	0.17±0.03^{a}	0.39±0.06^{a}	1.02±0.13^{b}	0.45±0.08^{a}	0.50±0.10^{a}	1.15±0.13^{b}
Total	4.02±0.58^{a}	5.09±0.48^{a}	10.40±1.17^{bc}	7.03±1.42^{ab}	13.77±1.73^{cd}	13.39±1.23^{cd}

Values are presented as mean±S.E.M. for 4 or 5 animals in each group. Total values are sum of six ceramide species. Different superscript letters indicate significant differences at $p<0.05$ (Tukey–Kramer *post hoc* test).

Table 2B. Levels of Ceramides in the Plasma of Wild-Type and ApoE$^{-/-}$ Mice

(B) Plasma ceramide levels (nmol/mL)

Plasma	7w WT	15w WT	65w WT	7w apoE$^{-/-}$	15w apoE$^{-/-}$	65w apoE$^{-/-}$
C16:0	0.53±0.04^{a}	0.50±0.09^{a}	0.47±0.05^{a}	5.63±0.42^{b}	4.33±0.26^{c}	3.34±0.39^{c}
C18:0	0.14 ± 0.03^{a}	0.20 ± 0.03^{a}	0.16 ± 0.02^{a}	0.82 ± 0.10^{b}	0.85 ± 0.05^{b}	0.47 ± 0.07^{c}
C22:0	1.06±0.12^{a}	0.98±0.15^{a}	0.79±0.06^{a}	8.50±1.12^{b}	6.61±0.44^{b}	3.77±0.26^{c}
C24:0	4.86±0.48^{a}	3.89±0.68^{a}	2.96±0.38^{a}	25.76±3.44^{b}	16.81±0.82^{c}	12.08±0.64^{c}
C24:1	2.82±0.46^{a}	3.20±0.55^{a}	2.33±0.24^{a}	14.84±1.90^{b}	12.93±0.58^{bc}	9.43±0.59^{c}
C24:2	0.20 ± 0.05^{a}	0.22 ± 0.04^{a}	0.21 ± 0.02^{a}	1.05 ± 0.05^{a}	1.01 ± 0.07^{ab}	1.37 ± 0.44^{b}
Total	9.62±1.14^{a}	8.99±1.48^{a}	6.92±0.72^{a}	56.60±6.54^{b}	42.53±1.81^{c}	30.46±1.74^{c}

Values are presented as mean±S.E.M. for 4 or 5 animals in each group. Total values are sum of six ceramide species. Different superscript letters indicate significant differences at $p<0.05$ (Tukey–Kramer *post hoc* test).

Table 2C. Levels of Ceramides in the Liver of Wild-Type and ApoE$^{-/-}$ Mice

(C) Liver ceramide levels (nmol/g tissue)

Liver	7w WT	15w WT	65w WT	7w apoE$^{-/-}$	15w apoE$^{-/-}$	65w apoE$^{-/-}$
C16:0	47.03±4.12^{a}	72.29±5.66^{b}	60.20±5.22^{ab}	52.47±4.87^{ab}	56.07±2.02^{ab}	55.09±3.71^{ab}
C18:0	8.03±0.85^{a}	16.48±2.15^{b}	13.10±0.29^{ab}	10.19±1.54^{a}	12.02±1.35^{ab}	8.07±0.98^{a}
C22:0	44.14±1.96^{a}	65.93±3.69^{b}	67.06±3.28^{b}	66.16±7.25^{b}	65.48±4.23^{b}	38.75±2.36^{a}
C24:0	128.87±5.43^{ab}	169.37±10.78^{a}	156.39±16.47^{ab}	178.40±19.69^{a}	153.40±6.30^{ab}	105.94±4.78^{b}
C24:1	201.38±11.52^{a}	283.16±13.98^{b}	239.44±12.91^{ab}	200.30±8.90^{a}	247.01±11.85 ^{ab}	208.74±10.94^{a}
C24:2	16.67±0.97	22.33±1.70	20.40±3.24	21.30±1.83	24.23±1.11	24.11±3.87
Total	446.12±22.95^{ac}	629.55±29.14^{b}	556.58±26.09^{ab}	528.82±35.68^{abc}	558.22±15.30^{ab}	440.69±19.06^{c}

Values are presented as mean±S.E.M. for 4 or 5 animals in each group. Total values are sum of six ceramide species. Different superscript letters indicate significant differences at $p<0.05$ (Tukey–Kramer *post hoc* test).